J Supercomput (2019) 75:704–718
https://doi.org/10.1007/s11227-017-2080-0

Medical image denoising using convolutional neural network: a residual learning approach

Worku Jifara[1] · Feng Jiang[1] · Seungmin Rho[2] · Maowei Cheng[3] · Shaohui Liu[1]

Published online: 1 June 2017

Abstract In medical imaging, denoising is very important for analysis of images, diagnosis and treatment of diseases. Currently, image denoising methods based on deep learning are effective, where the methods are however limited for the requirement of training sample size (i.e., not successful enough for small data size). Using small sample size, we design deep feed forward denoising convolutional neural networks by studying the model in deep framework, learning approach and regularization approach for medical image denoising. More specifically, we use residual learning as a learning approach and batch normalization as regularization in the deep model. Unlike most of the other image denoising approaches which directly learn the latent clean images, the residual learning approach learns the noise from the noisy images instead of the latent clean images where the denoised images are obtained by subtracting the learned residual from the noisy image. Moreover, batch normalization is integrated

✉ Feng Jiang
fjiang@hit.edu.cn

Worku Jifara
worku.jifara@gmail.com

Seungmin Rho
smrho@sungkyul.edu

Maowei Cheng
chengmaoweimm@126.com

Shaohui Liu
shliu@hit.edu.cn

1 School of Computer Science and Technology, Harbin Institute of Technology, Harbin, China

2 Department of Media Software, Sungkyul University, Anyang, Korea

3 College of Command Information System, PLA University of Science and Technology, Nanjing 150001, China

with residual learning to improve model learning accuracy and training time. We compute the quality of the reconstructed or denoised image in standard image quality metrics, peak signal to noise ratio and structural similarity and compare our model performance with some medical image denoising techniques. Experimental results reveal that our approach has better performance than some other methods.

Keywords Medical image · Image denoising · Residual learning · CNN · Batch normalization

1 Introduction

Medical images such as MRI, Mammograms, CT and ultrasound are subject to various types and degrees of noise, which might be happening during transmission and acquisition. The availability of noise in the medical images has direct or indirect influence that complicates the diagnosis, analysis and treatment process timely [1]. Also, the denoising process is disturbing the quality of the original image which may lead to poor decisions either by humans or machines. Therefore, the goal of noise removal or reduction in the medical image should take high consideration about accuracy as much as possible.

Image denoising being a conventional problem in the field of computer vision and has been extensively studied by researchers. Transform based, such as discrete wavelet (DW) [2–4], Shearlet [5], curvelet [6], discrete cosine (DC) [7], isotropic diffusion filtering [8], bilateral filters [9] are the most widely studied and conventional medical image denoising techniques. In these techniques, signals can be well estimated by a linear combination of few basis elements (i.e., the signals are sparsely approximated in transform domain), where scarce high-magnitude transform coefficients are retained and the rest are rejected due to certain noise. Using sparse model, [10] proposed sparse 3-D (BM3D) transform by grouping similar 2-D image fragments (e.g., blocks) into 3-D data arrays, which is based on enhancing sparse representation in the transform domain. Also, [11] introduced sparse and redundant representation over learned dictionaries where the proposed algorithm at once train a dictionary on its corrupted content using K-SVD, and its computational complexity is one of the algorithm shortcoming.

With the recent development of deep learning [12–14], the results from deep architecture have been showing a great performance. Denoising autoencoder [15] and convolutional denoising autoencoders (CNN DAE) [16] are an extension of classical autoencoder and are extensively studied for medical image denoising. The model attempted to learn the denoised image from its noisy version by some stacked layers, but they are not robust enough to variation in noise types beyond what it has seen during training [17]. To address this problem, adaptive multicolumn deep neural network [18] was exploited for image denoising by computing optimal column weights through solving a nonlinear optimization problem and training independent network to approximate the optimal weight. Like this, the model avoids the necessity to determine the type of noise. Likewise, plain neural network [19] was attempted to denoise an image by learning a mapping which approximate noise free image from noisy image by plain multilayer perceptron applied to image patches. All the above methods have

a common formulation,

$$z = x + v \tag{1}$$

where z is the noisy image generated as a combination of image x and some noise v, all having image units. Following this formulation, most existing image denoising techniques attempt to approximate the clean image x from a noisy observation z. Very recently, [20] proposed image denoising model using residual learning of deep convolutional neural network (DnCNN) has provided promising performance among the states of the art. The model tries to approximate the noise v instead of the image x in (1), such that the approximated clean image $\hat{x}$ can be obtained as,

$$\hat{x} = z - \hat{v} \tag{2}$$

where $\hat{v}$ is the approximated residual (noise) by the model from the noisy observation z .

Using deep learning methods, it has been explained that, deep architecture can provide a competitive result if the model is able to be trained with very large data size [21–23]. That is, to provide better performance of a model, the techniques require large dataset, which is a serious problem when it comes to medical images, where obviously limited datasets are available. Therefore, in addition to seeking for appropriate denoising techniques, exploiting the deep learning application to image processing problems (for example denoising) with small dataset, like medical image is still an open research area.

Following [20], with our own modified architecture, this paper proposes medical image denoising model based on convolutional neural network with residual learning approach. Initially, the model tries to approximate the residual from the noisy observation. Then, different from [20] we multiply the learned residual by a very small constant number r ($r = 0.0001$) and add to the approximated residual to better approximate the residual. Then finally, the denoised image is obtained by subtracting the residual from the noisy observation as shown in Fig. 2. To improve the model accuracy and training speed, we incorporate batch normalization in the residual learning process. Our proposed medical image denoising model is illustrated in Fig. 1. The contribution of our work can be summarized as follows:

1. We develop medical image denoising model that benefits over small training dataset.
2. We design a deep feed forward convolutional neural network model which directly approximate the noise from a noisy image. Residual learning is used as learning algorithm, and batch normalization is also incorporated to boost model performance.
3. It is a pioneer model that denoise the medical image with residual learning approach.

The rest of the paper is organized as follows. Section 2 explains proposed architecture and some preliminaries concepts, experimental results are elaborated in Sect. 3, and finally Sect. 4 provides conclusion of the paper.

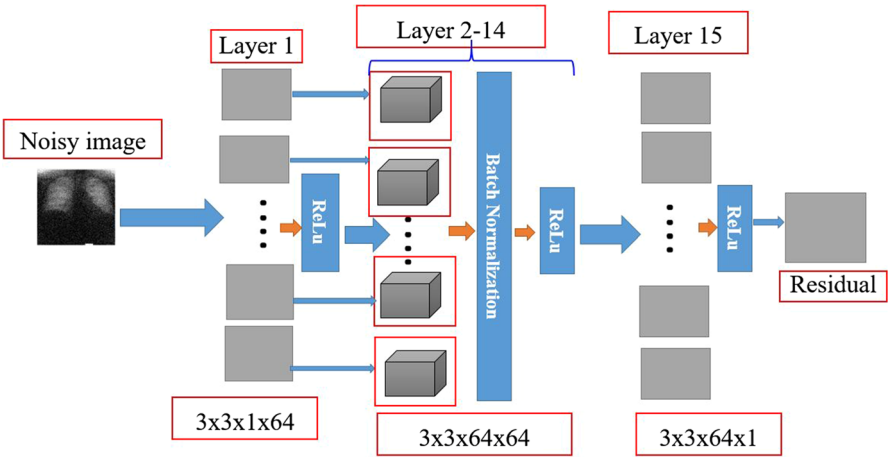

Fig. 1 Residual learning phase of the model for medical image denoising

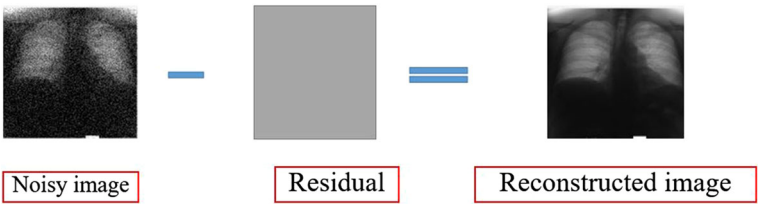

Fig. 2 Reconstruction phase of our model

2 Preliminary and proposed model

In this section, we have described some of the preliminaries of our medical image denoising technique and the proposed method.

2.1 Residual learning

Network depth is crucially necessary for classification problem. For example, many visual recognition tasks [12,24,25] have been seen that they are highly benefited from very deep network. However, as the depth increases the problem of vanishing or exploding gradient [26] is introduced which hinder convergence from the beginning. To address this issue, batch normalization [27] has been introduced to enable the network to converge for stochastic gradient descent (SGD) with back propagation. On the other hand, when deep network starts converging with batch normalization, a degradation problem is exposed, i.e., accuracy saturated and degrades rapidly which is not because of overfitting. To overcome with the above-stated problem (i.e., the degradation problem), the residual learning approach [28] along with some other approaches has been introduced.

The formulation of residual learning is as follows. Assume that $\Im(x)$ is considered as a mapping that fit the input x with some stacked layers [29,30]. The residual learning approach is that, rather than approximating $\Im(x)$ by stacked layers, its fine to approximate a residual function $\Re(x)$ as,

$$\Re(x) = \Im(x) - x \tag{3}$$

The original function $\hat{x}$ thus becomes,

$$\hat{x} = \Re(x) + x \tag{4}$$

As explained in [28,31] and verified with our experiments, the residual learning approach using convolutional neural network dramatically improves the model accuracy and performance. For this reason, we consider the merits of residual learning for convolutional neural network and exploit the residual learning approach for medical image denoising.

2.2 Batch normalization

Considering the excellence of batch normalization for convolutional neural network, we incorporate batch normalization for medical image denoising, where batch normalization is explained hereunder.

Assume that $x = \{x_1, x_2, \ldots, x_d\}$ is the input (batch of images) to the first layer of a model with dimension d .Then, each dimension of x is normalized by

$$\hat{x}_k = \frac{x_k - \mathrm{E}(x_k)}{\sqrt{\mathrm{Var}[x_k]}} \tag{5}$$

where $\mathrm{E}(x_k)$ is an expectation of x_k and $\mathrm{Var}[x_k]$ is the variance of x_k, and they are computed over the training data. This type of normalization speedup convergence [27], even when the features are not decorrelated. Normalizing each input in the layer may sometimes change what really the layer should represent. To address this problem, the transformation inserted in the network is chosen to be an identity transform. For this matter, a pair of parameters γ_k and η_k for each x_k have been introduced to scale and shift the normalized value as:

$$y_k = \gamma_k \hat{x}_k + \eta_k \tag{6}$$

where γ_k and η_k are learned along with the model parameters. In such manner or formulation, convolutional neural network model is benefited from batch normalization. Batch normalization helps the network train faster and provides higher accuracy. Figure 3 shows the test accuracy of MNIST network after batch normalization is incorporated in the model that is taken from [27]. The red solid line represents the higher accuracy achieved with batch normalization, and the blue dotted line represents the model accuracy without batch normalization and which implies the lower performance of the model. For our medical image denoising, we found that incorporating batch normalization between convolution layer and ReLu activation function boost the accuracy

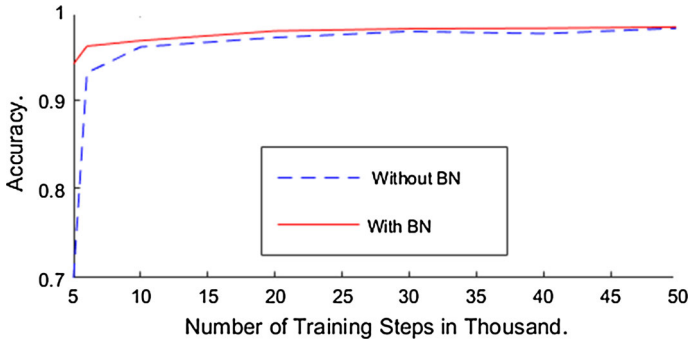

Fig. 3 The test accuracy of the MNIST network trained with and without batch normalization, versus the number of training steps

of the model and make the training process faster where ReLu is an activation function defined as,

$$f(x) = \max(0, x) \tag{7}$$

2.3 Autoencoder and its variations

An autoencoder takes an image (patch) $x \in R^d$ as input and first map it to a hidden representation $y \in R^d$ through a function,

$$y = s(wx + b) \tag{8}$$

where s is a nonlinearity activation function (such as sigmoid, ReLu), w and b are weight and bias, respectively. The hidden representation y is then mapped back into something resembling original image x by,

$$z = s(\grave{w}x + \grave{b}) \tag{9}$$

The parameters $\{w, \grave{w}, b, \grave{b}\}$ are optimized by minimizing an appropriate cost function.

Denoising autoencoder force the model to learn reconstruction of input given its noisy version which is an extension of classical autoencoder. More formally, let $x_i (i = 1, 2, \ldots, N)$ be the original image and $y_i (i = 1, 2, \ldots, N)$ be the corresponding noisy version of each x_i, then denoising autoencoder can be formulated as,

$$h(y_i) = s(wx_i + b) \tag{10}$$

$$\hat{x}(y_i) = s(\grave{w}h(x_i) + \grave{b}) \tag{11}$$

where h_i is the hidden layer activation, $\hat{x}(y_i)$ an approximation of y_i and $\{w, \grave{w}, b, \grave{b}\}$ are still parameters to be optimized by appropriate cost function.

Convolutional autoencoder is still an extension of conventional autoencoder, and they are differing from autoencoder as their weights are shared among all location [32–34] in the input, to preserve spatial locality. Currently, medical image denoising based

on convolutional autoencoder had better performance than the denoising autoencoder and autoencoder. Therefore, we compared our results with this currently published medical image denoising based on convolutional denoising autoencoder [16] and also with others where we observed the better performance of our method.

2.4 Proposed medical image denoising

2.4.1 The proposed method formulation

Consider the classical formulation of image denoising given as in Eq. (1). To predict the latent clean image from z, most of others denoising methods learn the mapping function,

$$\Im(z) \approx x \tag{12}$$

For medical image denoising, we follow [20] and residual learning formulation to learn residual mapping,

$$\Re_1(z) \approx v \tag{13}$$

and the original function thus becomes,

$$\hat{x} = z - \Re_1(z) \tag{14}$$

Even if the learned residual $\Re_1(z)$ is optimized by our defined cost function, we have observed that the residual approximated by our model could not fully extract the noise from the noisy image(i.e., there is lack in residual optimality). To better approximate the learned residual, we made two kind of experiment: (i) we multiply small constant number $r = 0.0001$ with the estimated residual and then add with the learned residual itself to get new approximated residual (ii) we multiply the same constant number with learned residual and subtract form the learned residual itself to get again new residual. Now, with the second experiment, our experimental results demonstrate that no improvement in PSNR values on reconstructed images, but with the first experiment, the model improves the PSNR values of the reconstructed images, which means the new residual is a better approximation. Therefore, our approach solves the problem of residual optimality in [20] and also gives better performance than [20] for medical image denoising. To easily represent in mathematical form, we multiply the first estimated residual with a chosen constant number r to generate a next residual $\Re_2(z)$, i.e.,

$$\Re_2(z) = r\Re_1(z) \tag{15}$$

Then, we combine $\Re_2(z)$ with $\Re_1(z)$ together to improve the learned residual quality and finally, the original function (denoised image) becomes,

$$\hat{x} = z - \Re_1(z) - \Re_2(z) \tag{16}$$

To learn the trainable parameters, the loss function between the desired residual image $\{(z_k - x_k)\}$ and estimated one $\{\Re(z_k; \lambda)\}$ is adopted and formulated as

$$l(\lambda) = \frac{1}{2N} \sum_{k=1}^{N} \| \Re(z_k; \lambda) - (z_k - x_k) \|_F^2 \tag{17}$$

where λ denotes trainable parameters, $\{z_k, x_k\}_{k=1}^{N}$ are N noise-clean training image (patch) pairs and $\|.\|_F^2$ is Frobenius norm and for a matrix A, it is given by,

$$\| A \|_F^2 = \sum_{i,j} |a_{ij}|^2 \tag{18}$$

2.4.2 Model architecture details

The model architecture has 15 layers depth and trained by minimizing the cost function in Eq. (17). As we have shown our model architecture in Fig. 1, first in layer one, 64 filters of size $3\times3\times1$ are used to generate 64 feature maps from noisy image where 3×3 is the convolutions height and width, respectively, applied on the input image and 1 is image channel, which is gray-scale image and therefore 1 in our case. This layer is finally followed by ReLu activation function. Then, each 2–14 layer (hidden layers) has 64 filters of size $3\times3\times64$ to generate again 64 feature maps followed by batch normalization and then by ReLu activation function. Finally, layer 15 has 1 filter of size $3\times3\times64$ convolution followed by ReLu is used to produce the residual image, where the denoised image then generated by subtracting the learned residual by the model from the noisy image as shown in Fig. 2. Generally, in our model, the residual learning adopted is to learn the mapping $\Re(z)$ and batch normalization is incorporated between convolution and ReLu to lift up the model accuracy and speedup the training performance. The combination of batch normalization and Residual learning gradually identifies image structure from the noisy observation through hidden layers and introduced small constant parameter r. It was seen that the residual learning adopted has promising advantage for training deep network and further improves the network accuracy.

3 Experimental results and setting

3.1 Training and testing data

We train the model for Gaussian denoising with noise level $\sigma = 15$ and $\sigma = 25$ independently. To train the model, first we considered the image of chest radiographs with nodule and non-nodule from Japan Society of Radiological Technology (JSRT) database. This is a publicly available database with 247 PA chest radiographs collected from 13 institutions in Japan and one in the USA. Among 247 images, the size of 235 images is adjusted to 64×64 and 180×180 size for training. We used 64×64 image size to easily compare our result with [12] and 180×180 image size to further analyze

Table 1 The average result of our medical image denoising model, where i.s is image size, i.s.s is image sample size, and b.s is batch size

Noise level	Methods			
	Metrics	BM3D	DnCNN	Proposed
Model trained on i.s 180×180, i.s.s 547 and b.s 10				
15	PSNR	40.018	41.017	41.018
	SSIM	–	0.961	0.962
25	PSNR	37.265	38.594	38.584
	SSIM	–	0.932	0.931

Table 2 The average result of our medical image denoising model, where i.s is image size, i.s.s is image sample size, and b.s is batch size

Noise level	Methods		
	Metrics	DnCNN	Proposed
Model trained on i.s 64×64, i.s.s 235 and b.s 10			
15	PSNR	39.246	39.250
	SSIM	0.950	0.950
25	PSNR	36.696	36.70
	SSIM	0.932	0.932

Table 3 The average result of our medical image model, where i.s is image size, i.s.s is image sample size, and b.s is batch size

Noise level	Methods			
	Metrics	BM3D	DnCNN	Proposed
Model trained on i.s 180×180, i.s.s 547 and b.s 128				
15	PSNR	40.018	41.116	41.217
	SSIM	–	0.963	0.963
25	PSNR	37.265	38.871	38.882
	SSIM	–	0.949	0.959

our model and give comparison with other methods. For testing, we have randomly chosen 12 images among the 247 images, which are not included during training.

Second, we mixed 235 images from JSRT and 312 images from mini-MIAS database of Mammograms (a database with 322 images of 1024×1024 resolution) and adjusted the size to 180×180 to train the model. Finally, 22 randomly selected images from the two datasets (10 from Mammograms and 12 from chest radiographs) which are not included during training are used for testing the model. Experimental results reveal that our model is benefitted from increasing sample size of an image and large batch size, as can be seen in Tables 1, 2, 3 and 4. Figures 4, 5, 6, 7, 8 and 9 show the randomly selected images reconstructed by the model trained with large training sample size and batch size.

3.2 Training parameters

To capture sufficient spatial information of the image, we set network depth to 15 composed of layer of convolution, ReLu and batch normalization. We initialize the

Table 4 The average result and comparison of our medical image denoising model with different methods, where i.s is image size, i.s.s is image sample size, and b.s is batch size

Noise level	Methods			
	Metrics	CNN DAE	DnCNN	Proposed
Model trained on i.s 64×64, i.s.s 235 and b.s 10				
15	PSNR	–	39.246	39.250
	SSIM	0.89	0.950	0.950
25	PSNR	–	36.696	36.70
	SSIM	0.89	0.932	0.932

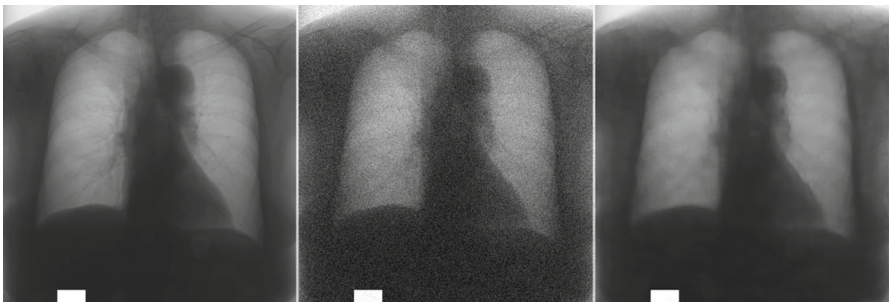

Fig. 4 (Chest radiography) model performance trained with 64×64 image size. The *first column* is the original image, the *second column* is the noisy image, and the *third column* is denoised image with $\sigma = 15$

Fig. 5 (Chest radiography) model performance trained with 64×64 image size. The *first column* is the original image, the *second column* is the noisy image, and the *third column* is denoised image with $\sigma = 25$

weights by the method in [35] and use Adam [36] algorithm with $\alpha = 0.01$, $\beta_1 = 0.9$, $\beta_2 = 0.999$ and $\epsilon = 10^{-8}$. The batch size is set to 10 (to give the comparison with CNN DAE) and 128 for the other. We have trained the model for 50 epochs. The learning rate is decayed exponentially from 0.01 to 0.0001 for the 50 epochs. We use the MatConvNet package [37] to train the proposed network. We also used data augmentation (clipping and rotation) for training the model. All experiments are carried out in the MATLAB (R2015b) environment running on a computer with Intel(R) Xeon(R) CPU E3-1230v3 3.30GHz and NVIDIA Tesla K40c GPU.

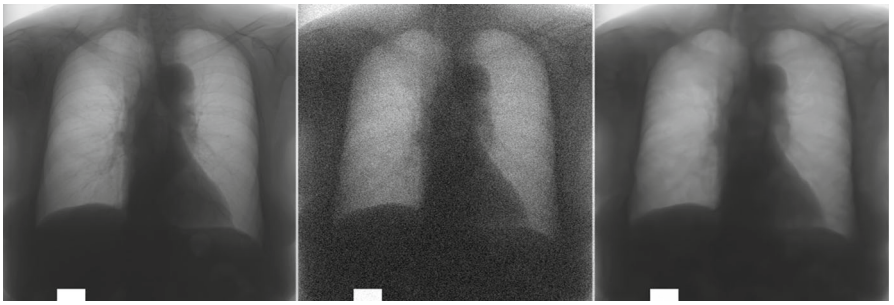

Fig. 6 (Chest radiography) model performance trained with 180×180 image size. The *first column* is the original image, the *second column* is the noisy image, and the *third column* is denoised image with $\sigma = 15$

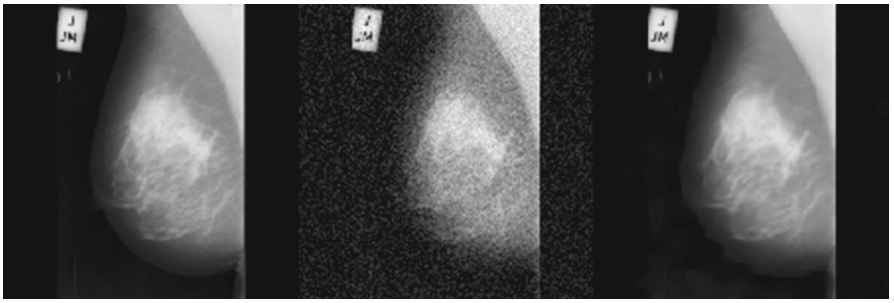

Fig. 7 (Mammograms image) model performance trained with 180×180 image size. The *first column* is the original image, the *second column* is the noisy image, and the *third column* is denoised image with $\sigma = 15$

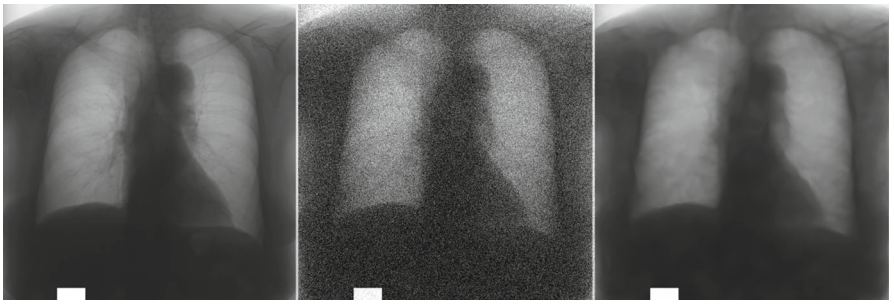

Fig. 8 (Chest radiography) model performance trained with 180×180 image size. The *first column* is the original image, the *second column* is the noisy image, and the *third column* is denoised image with $\sigma = 25$

3.3 Comparison with state-of-the-art algorithms

In this section, we are mentioning both qualitative and quantitative analysis of our model performance as in [38,39]. In qualitative analysis, we analyze our method based on different parameters, where as in quantitative analysis, we compare our results with other medical image denoising methods. We leave the qualitative comparison with other state of the art, because it is not feasible to evaluate with our eyes.

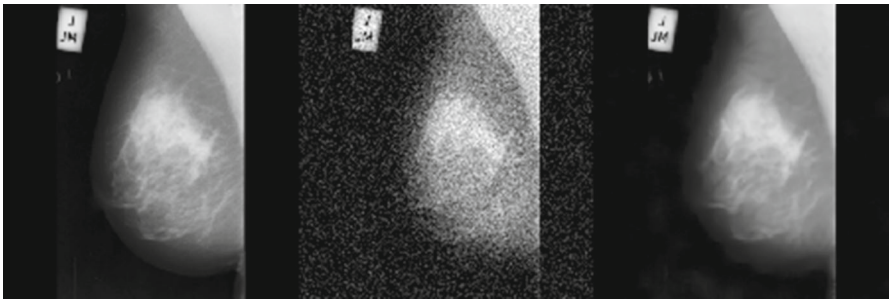

Fig. 9 (Mammograms image) model performance trained with 180×180 image size. The *first column* is the original image, the *second column* is the noisy image, and the *third column* is denoised image with $\sigma = 25$

3.3.1 Qualitative comparison

Qualitatively, we investigate our proposed method based on training sample size, image size used for training and batch size. The comparisons are illustrated in Figs. 4, 5, 6, 7, 8 and 9 with different parameters. Accordingly, Figs. 4 and 5 show the evaluation of our model trained on image sample size of 235 (chest radiographs image) of each size 64×64. They are randomly selected among the images used for testing the model. From the two figures, the reconstructed image is almost similar to the original image, where Fig. 4 is more similar to the original image because of low noise (i.e., $\sigma = 15$) in the image.

On the other hand, Figs. 6 and 7 represent the evaluation of our model trained on image sample size 547 of two different randomly selected among the test images of the same noise level, the same image size and the same batch size. In terms of noise level, in comparison with Fig. 4, these reconstructed images are better similar to the original image, which implies our model is benefited from large data size, image size and batch size. Also, we have observed similar conclusion by comparing Figs. 8 and 9 with Fig. 5 (i.e., image with same noise level)

3.3.2 Quantitative comparison

Quantitatively, first, we compared our model performance at different image size, training sample size and batch size. In Table 1, the average result of proposed model trained on image size 180×180, training sample size 547 images and batch size 10 is shown. It can be seen that the proposed model is better than DnCNN and BM3D at low noise level and outperforms at high noise level over DnCNN. But by changing only the batch size to 128, the proposed model become better in PSNR value as can be shown in Table 3. The model improves the reconstructed image quality by 0.101 dB over DnCNN and 1.199 dB over BM3D at $\sigma = 15$ and 1.617 dB over BM3D and 0.011 dB over DnCNN at $\sigma = 25$ in terms of PSNR value. Also, Table 2 exhibits the model performance with image sample size 235 of each 64×64 size and batch size 10. Again, it can be seen that our model has low PSNR and SSIM compared to the model

trained with large sample size and batch size but still better result in PSNR value and same value in SSIM.

Second, the comparison of our model with DnCNN and CNN DAE is shown in Table 4 both in PSNR and SSIM. To compare our model, we fixed our model trained with image size 64x64, training sample size 235 images and batch size 10. Accordingly, in PSNR image quality metric, the proposed model improves the average reconstructed image quality by 0.004 dB over DnCNN at both $\sigma = 15$ and $\sigma = 25$, whereas in SSIM image quality metric, the model improves the average reconstructed image quality by 0.06 dB at $\sigma = 15$ and 0.042 dB at $\sigma = 25$ over CNN DAE and similar value over DnCNN.

4 Conclusion and future work

An efficient deep convolutional neural network model for denoising of medical images for small training dataset is proposed in this paper. Unlike most of medical image denoising approaches which approximates the latent clean image from noisy observation, our model approximates the noise from the noisy observation. By combining residual learning and batch normalization, we speedup the training process and also increase the denoising performance of the model. Even though deep architecture has better performance with large training dataset, our medical image denoising model is trained with small dataset and achieves competitive results. With small training dataset, our experimental results demonstrate that the performance of the proposed medical image denoising model is better than the existing medical image denoising techniques both in Peak signal to noise ratio (PSNR) and structural similarity (SSIM). As we attempted to explain in the introduction, medical image is subject to various types of noise. For example, to manage the band size of medical images, images are compressed with different compression techniques (e.g., JPEG compression). While transmission band size is saved by compression, the compressed image is distorted with some noise, which is called compression artifact. This introduces noise in the medical image due to compression that may lead to poor decision making by humans as well as by machines. Therefore, in our future work we plan to investigate the compression artifact reduction of medical image with the current powerful convolutional neural network model.

Acknowledgements This work is partially funded by the MOE-Microsoft Key Laboratory of Natural Language Processing and Speech, Harbin Institute of Technology, the Major State Basic Research Development Program of China (973 Program 2015CB351804) and the National Natural Science Foundation of China under Grant Nos. 61572155, 61672188 and 61272386. We would also like to acknowledge NVIDIA Corporation who kindly provided two sets of GPU. We would like to acknowledge the editors and the anonymous reviewers whose important comments and suggestions led to greatly improved the manuscript.

References

1. Gao Q, Olgac N (2016) Determination of the bounds of imaginary spectra of LTI systems with multiple time delays. Automatica 72:235–241
2. Mondal T, Maitra M (2015) Denoising and compression of medical image in wavelet 2D. Int J Recent Innov Trends Comput Commun 6:173–178

3. Mustafa N, Li JP, Khan SA, Giess M (2015) Medical image de-noising schemes using wavelet transform with fixed form thresholding. Int J Adv Comput Sci Appl 6:173–178
4. Bahendwar YS, Sinh GR (2012) Efficient algorithm for denoising of medical images using discrete wavelet transforms. Math Methods Syst Sci Eng 142:158–162
5. Zhang X (2015) Image denoising using shearlet transform and nonlinear diffusion. Proc Sci 20:033016
6. Starck JL, Cands EJ, Donoho DL (2002) The curvelet transform for image denoising. IEEE Tran Image Process 11(6):670–684
7. Hu J, Pu Y, Wu X, Zhang Y, Zhou J (2012) Improved DCT-based nonlocal means filter for MR images denoising. Comput Math Methods Med 2012:85–91
8. Sameh Arif A, Mansor S, Logeswaran R (2011) Combined bilateral and anisotropic-diffusion filters for medical image de-noising. IEEE Student Conf Res Dev SCOReD 2:420–424
9. Bhonsle D, Chandra V, Sinha GR (2012) Medical image denoising using bilateral filter. Int J Image Gr Signal Process 4:36–43
10. Dabov K, Foi A, Katkovnik V, Katkovnik V, Egiazarian K (2007) Image denoising by sparse 3-D transform-domain collaborative filtering. IEEE Trans Image Process 16:2080–2095
11. Elad M, Aharon M (2006) Image Denoising via learned dictionaries and sparse representation. Comput Vis Pattern Recogn 1:1063–6919
12. Bengio Y, Lamblin P, Popovici D, Larochelle H (2007) Greedy Layer-Wise training of deep networks. Adv Neural Inf Process Syst 19:153
13. Schmidhuber J (2014) Deep learning in neural networks: an overview. J Neural Netw 61:85–117
14. Tan Z, Wei H, Chen Y, Du M, Ye S (2016) Design for medical imaging services platform based on cloud computing. Int J Big Data Intell 3(4):270–278
15. Vincent P, Larochelle H, Bengio Y, Manzagol PA (2011) Extracting and composing robust features with denoising autoencoders. In: IEEE Student Conference on Research and Development, pp 1096–1103
16. Gondara L (2016) Medical image denoising using convolutional denoising autoencoders. In: IEEE Conference on Computer Vision and Pattern Recognition
17. Buades A, Coll B, Morel JM (2005) A review of image denoising algorithms with a new one. SIAM J Multiscale Model Simul A SIAM Interdiscip 4:490–530
18. Agostinelli F, Anderson MR, Lee H (2013) Adaptive multi-column deep neural networks with application to robust image denoising. Adv Neural Inf Process Syst 26:1493–1501
19. Burger HC, Schuler CJ, Harmeling S (2012) Image denoising: can plain neural networks compete with BM3D? In: IEEE Computer Society Conference on Computer Vision and Pattern Recognition, pp 2392–2399
20. Zhang K, Zuo W, Chen Y, Meng D, Zhang L (2016) Beyond a Gaussian denoiser: residual learning of deep CNN for image denoising, Tech report Computer Vision and Pattern Recognition, pp 1–13
21. Girshick NR (2015) Fast R-CNN. Int Conf Comput Vis Pattern Recogn 1440–1448 (arXiv:1504.08083)
22. Girshick R, Donahue J, Darrell T, Malik J (2014) Rich feature hierarchies for accurate object detection and semantic segmentation. In: Proceedings of the IEEE Computer Society Conference on Computer Vision Pattern Recognition, pp 580–587
23. Oliveira TP, Barbar JS, Soares Alexsandro Santos (2016) Computer network traffic prediction: a comparison between traditional and deep learning neural networks. Int J Big Data Intell 3(1):28–37
24. Krizhevsky A, Sutskever I, Geoffrey EH (2012) Imagenet classification with deep convolutional neural networks. Adv Neural Inf Process Syst 25:1097–1105
25. He K, Zhang X, Ren S, Sun J (2014) Spatial pyramid pooling in deep convolutional networks for visual recognition. In: European Conference on Computer Vision, Springer, Berlin
26. Glorot X, Bengio Y (2010) Understanding the difficulty of training deep feedforward neural networks. In: Proceedings of the International Conference on Artificial Intelligence and Statistics vol. 9, pp 249–256
27. Ioffe S, Szegedy C (2015) Batch normalization: accelerating deep network training by reducing internal covariate shift. In: Proceedings of the 32nd International Conference on Machine Learning, pp 448–456
28. He K, Zhang X, Ren Sh, Sun J (2015) Deep residual learning for image recognition. In: Proceedings of the IEEE Conference on Computer Vision Pattern Recognition, pp 770–778 (arXiv preprint arXiv:1512.03385)
29. Xing C, Ma L, Yang X (2016) Stacked denoise autoencoder based feature extraction and classification for hyperspectral images. J Sens 2016:1–10. doi:10.1155/2016/3632943
30. Masci J, Meier U, Ciresan D, Schmidhuber J (2011) Stacked convolutional auto-encoders for hierarchical feature extraction. Springer, Berlin

31. Jiang F, Rho S, Chen B, Du X, Zhao D (2015) Face hallucination and recognition in social network services. J Supercomput 71(6):2035–2049
32. Jiang F, Chen B, Li K, Zhao D (2014) Big data driven decision making and multi-prior models collaboration for media restoration. Multimedia Tools Appl 75:12967–12982
33. Jiang F, Chen BW, Rho S et al (2016) Optimal filter based on scale-invariance generation of natural images. J Supercomput 72(1):5–23
34. Jiang F, Ji X, Hu C, Liu S, Zhao D (2014) Compressed vision information restoration based on cloud prior and local prior. IEEE 2:1117–1127
35. He K, Zhang X, Ren S, Sun J (2015) Delving deep into rectifiers: surpassing human-level performance on imagenet classification. In: IEEE International Conference on Computer Vision pp 1026–1034
36. Kingma D, Ba J (2015) Adam: a method for stochastic optimization. Paper at the 3rd International Conference for Learning Representations
37. Vedaldi A, Lenc K (2015) Matconvnet: convolutional neural networks for matlab. In: Proceedings of the 23rd Annual ACM Conference on Multimedia Conference, pp 689–692
38. Chen BW, Wang JC, Wang JF (2009) A novel video summarization based on mining the story-structure and semantic relations among concept entities. IEEE Trans Multimed 11(2):295–312
39. Chen BW, Chen CY, Wang JF (2013) Smart homecare surveillance system: behavior identification based on state transition support vector machines and sound directivity pattern analysis. IEEE Trans Syst Man Cybern Syst 43(6):1279–1289